Thermal reshaping as a route for reuse of end-of-life glass fibre-reinforced acrylic composites

Thermal reshaping as a route for reuse of end-of-life glass fibre-reinforced acrylic composites

Winifred Obande [a], Danijela Stankovic [a], Ankur Bajpai [a], Machar Devine [a], Christian Wurzer [b], Anna Lykkeberg [c], Jennifer A Garden [c], Conchúr M. Ó Brádaigh [a], Dipa Ray [a, *]

[a] School of Engineering, Institute for Materials and Processes, The University of Edinburgh, Sanderson Building, Robert Stevenson Road, Edinburgh EH9 3FB, Scotland, United Kingdom

[b] School of GeoSciences, UK Biochar Research Centre, The University of Edinburgh, Edinburgh EH9 3FF, Scotland, United Kingdom

[c] EaStCHEM School of Chemistry, The University of Edinburgh, Joseph Black Building, David Brewster Road, Edinburgh EH9 3FJ, Scotland, United Kingdom

* Corresponding author. E-mail address: dipa.roy@ed.ac.uk (D. Ray)

ABSTRACT

Thermal reshaping has been employed to simulate the end-of-life reuse of liquid-resin-infused thermoplastic acrylic composite laminates, and the associated effects on matrix-dominated mechanical performance and microstructure have been studied. L-shaped laminates were infused at room temperature and subjected to 1 or 4 hot-press flattening cycles (25 min at 120°C; 11 bar). Compared to the original references, up to 13% higher transverse flexural strengths were measured for the reprocessed laminates. Such a scheme may be readily implemented for high-value reuse without sacrificing fibre length scales with 10-cycle and 15-cycle mass losses of only 2% and 2.6%, respectively. This study provides important insights to foster a greater understanding of the performance limits of hot-press reprocessing to inform the practical reuse and re-application of sustainable composites in a circular economy.

1. Introduction

Fibre-reinforced polymer (FRP) composites continue to be attractive subjects for research, production and use across many sectors, owing to their exceptional specific strength and stiffness properties, and excellent application-specific tailorability for diverse environments and loading conditions (e.g.: corrosion and fatigue). From a reprocessibility point of view, thermoplastic (TP) matrices are superior to their thermosetting (TS) counterparts, as their long polymer chains are not cross-linked, allowing for repeated melting and re-processing. High melt viscosities, however, were historically a major limiting factor to the widespread use of thermoplastic fibre-reinforced polymers (TP-FRPs). More recently, advanced innovative

reactive TP resin formulations have facilitated the fabrication of TP-FRPs using technologies that were once solely applicable to low-viscosity TS resins. In light of growing environmental concerns surrounding the depletion of fossil fuel resources, and the waste-related end-of-life legacy issues affecting several sectors, the timeliness of these advancements cannot be understated in enabling a shift from TS-FRPs, which are more challenging to reprocess [1]. Notwithstanding, sustainably meeting the demands posed by continued composites market growth will require rigorous counterbalancing measures such as minimising the dependence on finite resources while improving resource efficiency [2,3]. As it stands, a projected 25 billion metric tonnes of plastic waste will be generated by 2050 if such measures are not effectively established and developed [4].

Various recycling technologies have been demonstrated and the most applied methods broadly fall under three categories. (i) Mechanical recycling involves the grinding or shredding of fibre-reinforced polymer composites into smaller fragments or pieces to be reused by moulding. (ii) Pyrolysis involves the conversion of waste composite materials into gaseous volatiles, char, and recovered fibres by heating under inert atmospheres between 350°C and 800°C. (iii) Finally, solvolysis employs solvents (e.g.: supercritical fluids and catalytic solutions) as depolymerisation or bond-breaking media for fibre and matrix recovery [4–11]. Although mechanical recycling is widely applied due to the requirement for relatively low energy and the absence of harsh solvents, the reduction in fibre length scales can result in considerable losses of performance. Moreover, compared to pyrolysis, solvolysis can offer the advantage of requiring lower temperatures and producing clean, char-free fibre surfaces; however, the negative environmental and health impacts of solvents and catalysts may often outweigh the benefits [12].

As thermoplastic monomeric and oligomeric resins such as the Elium® family of acrylic resins by Arkema continue to grow in popularity, more and more research efforts have been invested in establishing a comprehensive database of performance and applicability [13–20]. While some recent works have been published addressing the gaps in end-of-life recycling and reuse [21–24], the effects of thermal reshaping on performance remain substantially unexplored except for previous research by Cousins et al. [24] where the reuse potential of large-scale acrylic-matrix composites was demonstrated by thermoforming among other techniques. Current waste management strategies are insufficiently developed, placing undue emphasis on the lower tiers of the waste hierarchy instead of prioritising value maximization. This will undoubtedly need to be addressed to offset current and future landfilling rates.

Reusing and repurposing end-of-life materials, e.g.: from decommissioned large-scale wind turbine blades provide attractive pathways for energy and resource recovery in line with the waste management hierarchy. Moreover, reuse via thermal reshaping bypasses the challenges associated with traditional fibre and matrix separation processes, as well as those emanating from the collection, sorting and realignment of reclaimed fibres [25]. Nonetheless, there is a considerable lack of published literature exploring the effects of thermal reshaping on residual performance. Such studies are essential in building a comprehensive performance database for improved reliability and confidence as drivers for the rapid adoption of high-value reused composites into the future.

Thus, this study aims to simulate and evaluate an end-of-life, hot-press-based reshaping and reprocessing scheme for applicability to glass fibre-reinforced acrylic composites to maximise the benefit of fibre length scales and enhance performance. To offer additional insights, dynamic thermogravimetric analysis (TGA), dynamic mechanical analysis, and solution-state nuclear magnetic resonance and size exclusion chromatography using gel permeation chromatography have been employed. Static and cyclic isothermal TGA has also been used to simulate prolonged and repeated thermal cycling.

2. Materials and methods

2.1. Materials

This work employed a liquid thermoplastic acrylic resin (Elium® 180 – Arkema GRL, France), *in situ* polymerised with a dibenzoyl peroxide initiator (BP-50-FT) supplied by United Initiators GmbH, Germany. Laminates comprised 4 plies $[90]_4$ of a glass fibre non-crimp fabric (TEST2594) supplied by Ahlstrom-Munksjö Glassfibre OY, Finland. The quasi-unidirectional fabric construction included glass fibres in the 0°- (600 g/m^2) and 90°- (36 g/m^2) directions, as well as PES stitching (10 g/m^2).

2.2. Laminate fabrication and thermal reshaping

2.2.1. Liquid resin infusion

L-shaped laminates were produced by liquid resin infusion at room temperature using a custom steel mould. 4 plies of glass NCF were used for a target thickness of 2 mm, with the 0° fibre axes coinciding with the seam line as indicated by the arrows in Figure 1 (Steps 2 – 6). Following resin infusion, the laminate was left to polymerise at room temperature for 24 h before demoulding.

2.2.2. Platen press reprocessing and reshaping

Once demoulded, the *L-shaped* laminate was trimmed as illustrated in Figure 1 (Step 2) to obtain a vertical height of 134 mm and target flattened dimensions of 380 mm [90°] × 280 mm [0°] as shown in Figure 1 – Step 3. Original reference samples were extracted from the offcuts of the *as-infused* laminate (Figure 1 – Step 2). These samples will hereafter be referred to as R×0 samples. Similarly, samples extracted after reprocessing once and four times are denoted R×1 and R×4, respectively.

Flattening was carried out by subjecting the laminates to a thermal cycle on a Pinette Emidecau Industries Heated Platen Press (Model: Lab 450 P), where the platens have been heated to 120°C. For Step 3 (Figure 1), a stepwise platen closure approach was adopted to produce the flattened components, with incremental closure every 5 minutes until the laminate had been flattened, as depicted in Figure 2. This was done to facilitate progressive chain relaxation within the thermoplastic polymer matrix and to prevent damaging the component under rapid loading. Finally, at full platen closure, the components were held at 120°C for a further 5 minutes at 11 bar consolidation pressure. The components were actively cooled (10°C/min) to 40°C while maintaining pressure and removed thereafter. Graphical overviews of the processing cycles are shown in Figure 2.

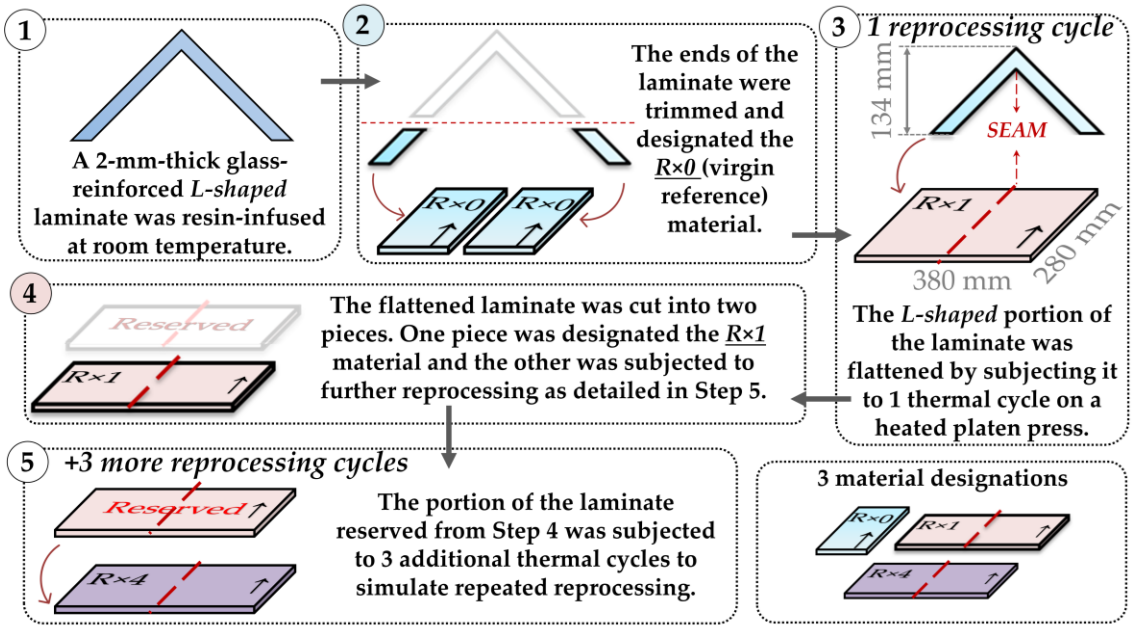

Figure 1. Graphical representation of the *L-shaped* laminate production and reprocessing sequence. The overlayed arrows on each laminate indicate the corresponding fibre directions.

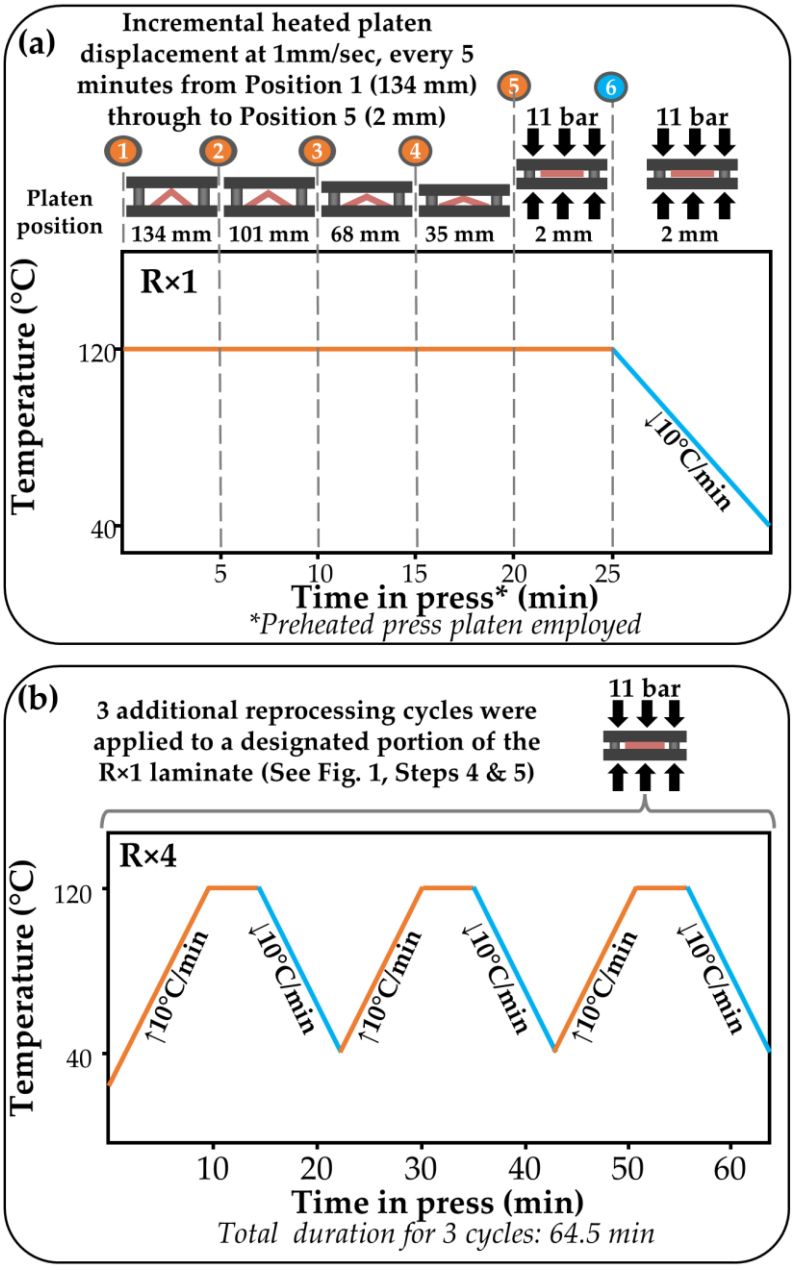

Figure 2. A graphical representation of the reprocessing cycle parameters employed for (a) R×1 and (b) R×4 laminates. Details of platen positions, temperatures and applied pressures are provided where applicable.

The fibre and void volume fractions for the R×0, R×1 and R×4 laminates were determined by the burn-off technique (ASTM D3171) and are summarised in Table 1 with corresponding thicknesses. Samples were extracted using a water-lubricated, diamond-coated saw blade and dried in a convection oven at 50°C overnight to remove residual moisture from the cutting process. Further details of test specimen preparation and characterisation techniques are provided in the corresponding sections.

Table 1. Summary of fibre and void volume fractions for virgin (R×0), and reprocessed (R×1 and R×4) glass fibre-reinforced acrylic (GF/A) samples determined using the resin burn-off method. Results were averaged from triplicates.

	GF/A (R×0)	GF/A (R×1)	GF/A (R×4)
Fibre volume fraction (%)	47.4 ± 0.7	47.9 ± 0.8	48.6 ± 0.4
Void volume fraction (%)	2.0 ± 0.3	2.0 ± 1.0	2.0 ± 0.3
Laminate thickness (mm)	2.15 ±0.04	2.10 ±0.04	2.10 ±0.06

2.3. Transverse flexural testing

Samples measuring 154 mm × 13 mm were extracted for the determination of transverse flexural properties (strengths and moduli) by three-point bending in accordance with ASTM D7264. A span-to-thickness ratio of 32:1, corresponding to sample lengths of 154 mm and a crosshead speed of 1 mm/min were employed. Loading nose and supports were hardened steel pins of 6 mm diameter. Testing was performed on an Instron (3369) test frame fitted with a 10 kN load cell (Instron 2530-10 kN) while mid-span deflections were tracked and recorded via non-contact video extensometery. An illustration of the extraction scheme for flexural test specimens is presented in Figure 3.

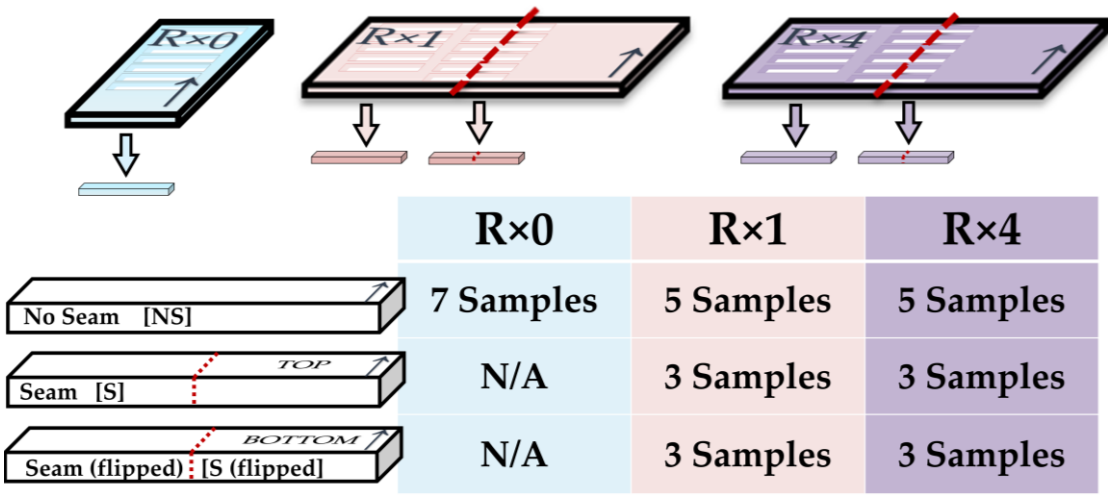

Figure 3. A graphical representation of the transverse flexural test sample extraction scheme for all conditions [R×0, R×1 and R×4] and all configurations [no seam and seam (flipped and unflipped)]. Test samples measured 154 mm × 13 mm × 2 mm.

2.4. Dynamic mechanical analysis (DMA)

Longitudinal test samples with nominal measurements, 60 mm × 10 mm were extracted from seam-free regions and subjected to DMA testing in accordance with BS ISO 6721-11 for the determination of thermomechanical properties. Note that samples were extracted from the seam-free regions of each

laminate, with the longitudinal axes coinciding with the fibre direction indicated by the arrow in Figure 3. A TA Instruments Discovery DMA 850 was used in three-point bending mode. Samples were heated from ambient temperature to 180°C at 3°C/min and dynamically loaded at a frequency of 1 Hz and an amplitude of 10 μm. Storage and loss moduli and tan delta were recorded as functions of temperature throughout testing. Three samples were tested for each condition (R×0, R×1 and R×4).

2.5. Thermogravimetric analysis

A Mettler Toledo TGA/DSC 1 analyser was used in this work in three ways. Firstly, dynamic thermogravimetric analysis (TGA) was used to assess the thermal stability and decomposition behaviour of the R×0, R×1, and R×4 materials in air by heating from ambient temperature to 800°C at a rate of 10°C/min. Secondly, the TGA instrument was used to simulate 15 successive reprocessing cycles with isothermal holds at 120°C for 60 min to determine the cumulative mass loss at Cycle 15; the total duration at 120°C is 900 min. Thirdly, the effect of prolonged heating (900 min) at 120°C on the evolution of mass loss was studied. For each TGA study type, samples weighing approximately 15 mg were analysed in duplicates.

2.6. Solution-state nuclear magnetic resonance (NMR) spectroscopy and size exclusion chromatography (SEC)

The polymer matrices from virgin (R×0) and reprocessed (R×1 and R×4) materials were analysed by NMR spectroscopy to investigate any change in the chemical structure due to degradation. Fibre-reinforced samples were immersed in chloroform to dissolve the matrix phase, and the glass fibres were removed by filtration. The solvent was subsequently evaporated to produce a transparent film of acrylic matrices. All samples were soluble in other common solvents, specifically acetone and tetrahydrofuran (THF). The chemical structures of the recovered matrix films for all conditions (R×0, R×1 and R×4) were compared using ^{1}H and 2D NMR experiments (Diffusion-Ordered SpectroscopY (DOSY)). NMR spectra were recorded on a Bruker AVA500 (USA) spectrometer (500 MHz) at 298 K in $CDCl_3$ and referenced to the residual $CDCl_3$ peak (^{1}H: δ 7.26 ppm).

For SEC analysis, the recovered polymer matrix was dissolved in Gel permeation chromatography (GPC) grade THF and filtered using a 0.2 μm PTFE syringe filter. Each sample was run at a flow rate of 1 mL min^{-1} at 35°C on a 1260 Infinity II GPC/SEC single detection system with two mixed bed C PLgel columns

(300 mm × 7.5 mm). Molecular weights were obtained based on a calibration curve of narrow molecular weight distribution polystyrene.

To provide insights for interpreting the results of mechanical testing, microscopic inspections were conducted on the cross-section of seam-containing R×1 and R×4 samples alongside an R×0 sample. Samples were cut in the direction transverse to the 0° fibres, with the cross-sectional region of interest along the cut plane as shown in Figure 4a. The micrographs revealed distinct characteristics in the reprocessed materials R×1 (Figure 4c) and R×4 (Figure 4d) from those in the virgin reference R×0 (Figure 4b).

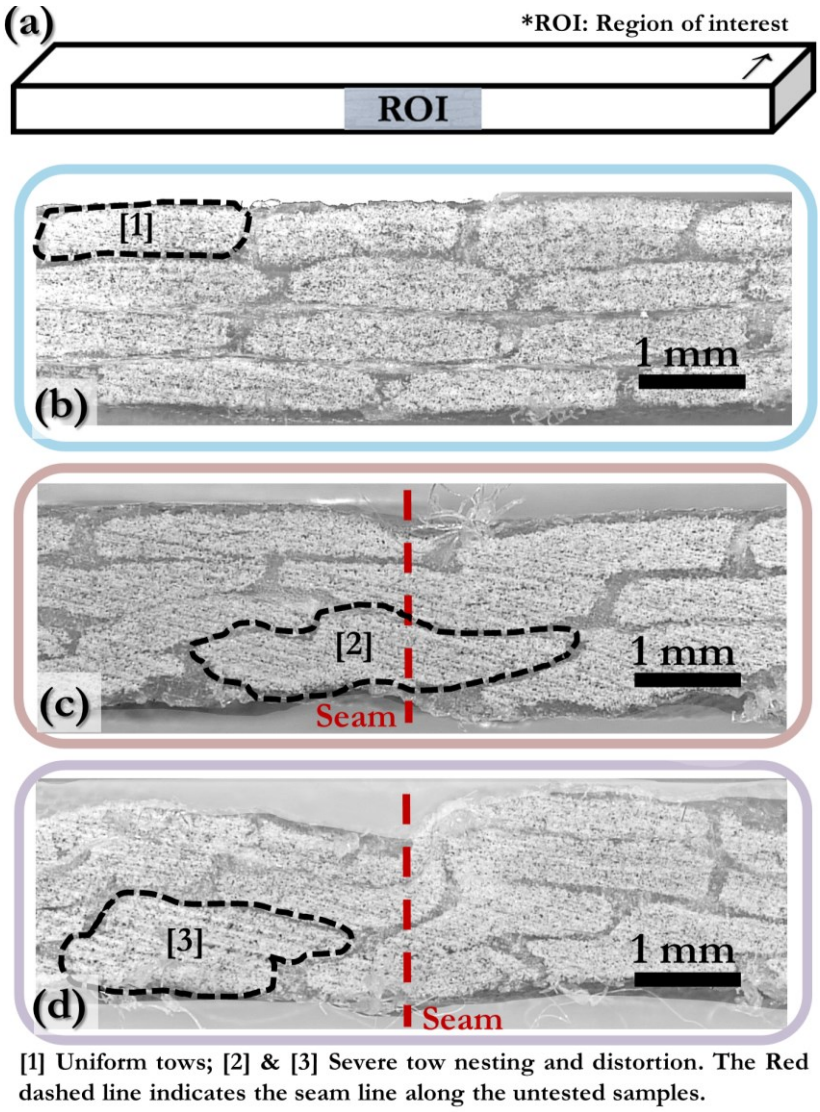

Figure 4. (a) A graphical representation of the region of interest (ROI) designated for cross-sectional microscopic inspections on glass fibre-reinforced acrylic samples after (b) 0, (c) 1, and (d) 4 reprocessing cycles. Note: samples were cut in the direction transverse to the 0° fibres. Fibre volume fractions for these materials in order of increasing reprocessing cycles are 47.4%, 47.9% and 48.6%.

Given that these micrographs were obtained from untested samples from each material, the observed surface undulations, tow nesting and distortions in R×1 (Figure 4c) and R×4 (Figure 4d) are associated with the thermal reshaping process. While the R×0 material appears to have similar sizes of ellipsoidal tows stacked uniformly with minor resin-rich gaps, the irregularities produced by tow form distortion and nesting result in the formation of some highly packed fibre zones interspersed with resin-rich zones.

3.1. Transverse flexural test results

Results obtained from *no seam* samples from R×1 and R×4 conditions (Figure 5) will be directly compared to the virgin/*as infused*, R×0 samples to quantify the residual performance after thermal processing and the effects of successive reprocessing operations. Unflipped *seam* samples (as defined in Figure 3) will be directly compared with *no seam* samples within the same condition (R×1 or R×4) to gain insights into the effects of seam inclusion during thermal reshaping for the reuse of curved structures. Similarly, the comparisons between unflipped and flipped *seam* samples are intended to inform on the effects of primary form/shape and hot-press reprocessing on structural integrity and function during the secondary (R×1) and quinary (R×4) re-application of these materials.

3.1.1. The effects of the number of processing cycles on flexural properties

Figure 5 shows the transverse flexural stress-strain curves for the virgin R×0 samples (Figure 5a), the reprocessed R×1 (Figure 5b) and R×4 (Figure 5c) samples. All samples exhibit similar linear elastic regions in terms of the evolution of stress with strain, with varying extents of minor load drops (from damage development) leading up to failure. R×1_NS-2, -4, and -5, however (Figure 5b), had slightly higher strengths and failure strains (~3%). This may be due to more 0° tows remaining intact within these samples during damage evolution, resulting in the retention of load-bearing capacity between 1% and 3% strain. In addition, R×1 samples, particularly R×1_NS-1 (Figure 5b) exhibited a more distinct damage initiation point before the damage evolution region. The damage evolution behaviour of all samples suggests the occurrence and development of fragmentation and delamination processes, with more extensive damage occurring in R×1_NS samples.

It can also be observed that hot-press reprocessing results in an increase in both flexural strength and modulus as shown in Figure 5d, where the R×1 material exhibited 13% and 9% higher mean strength and modulus than those measured for its R×0 counterpart (77.1 MPa and 7.2 GPa), respectively. However,

when compared using an unpaired, one-tailed, two-sample Welch t-test with a significance level of 0.05 (refer to S1.3), it was found that only the strength value was statistically significant at $p < 0.05$.

Interestingly, a similar increase in flexural performance was reported for thermally aged (annealed) carbon fibre-reinforced acrylic composites by Bhudolia et al. [13], who ascribed this improvement to the positive effects of thermally-induced polymerisation of trapped monomeric residues within the composite laminates. However, the absence of discernible changes in matrix chemistry between R×0, R×1 and R×4 as discussed in Section 3.4 suggests the influence of other factors. In general, transverse direction performance is dominated by matrix and fibre-matrix interfacial properties [26,27]; thus, taken together with the NMR and SEC results in Section 3.4, the changes in laminate thickness between R×0 (2.15 ± 0.04 mm), R×1 (2.1 ± 0.4 mm) and R×4 (2.1 ± 0.6 mm) suggest that the reprocessing route employed herein may enhance fibre/matrix adhesion and enables more effective load transfer [28].

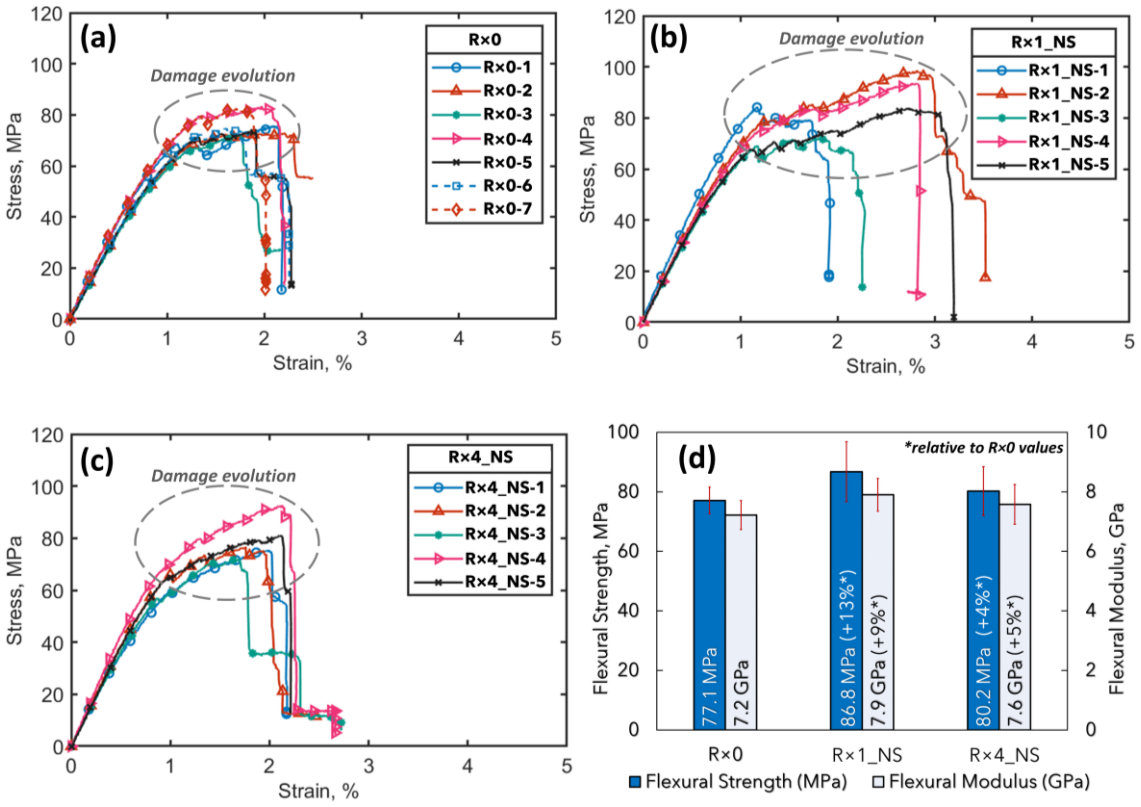

Figure 5. Transverse flexural stress-strain curves showing the effects of reprocessing cycles on glass fibre-reinforced composites where the # "R×#" indicates the number of reprocessing cycles employed in (a) R×0, (b) R×1, and (c) R×4; and (d) average transverse flexural strengths and moduli for these materials. Fibre volume fractions for these materials in order of increasing reprocessing cycles are 47.4%, 47.9% and 48.6%.

3.1.2. The effects of seam inclusion and orientation on flexural properties

Figure 6 presents direct comparisons of the flexural properties of seam-containing samples with their seam-free counterparts. Depending on the presence and orientation of seams with respect to applied loads, reprocessed components can exhibit considerable reductions in strengths and moduli.

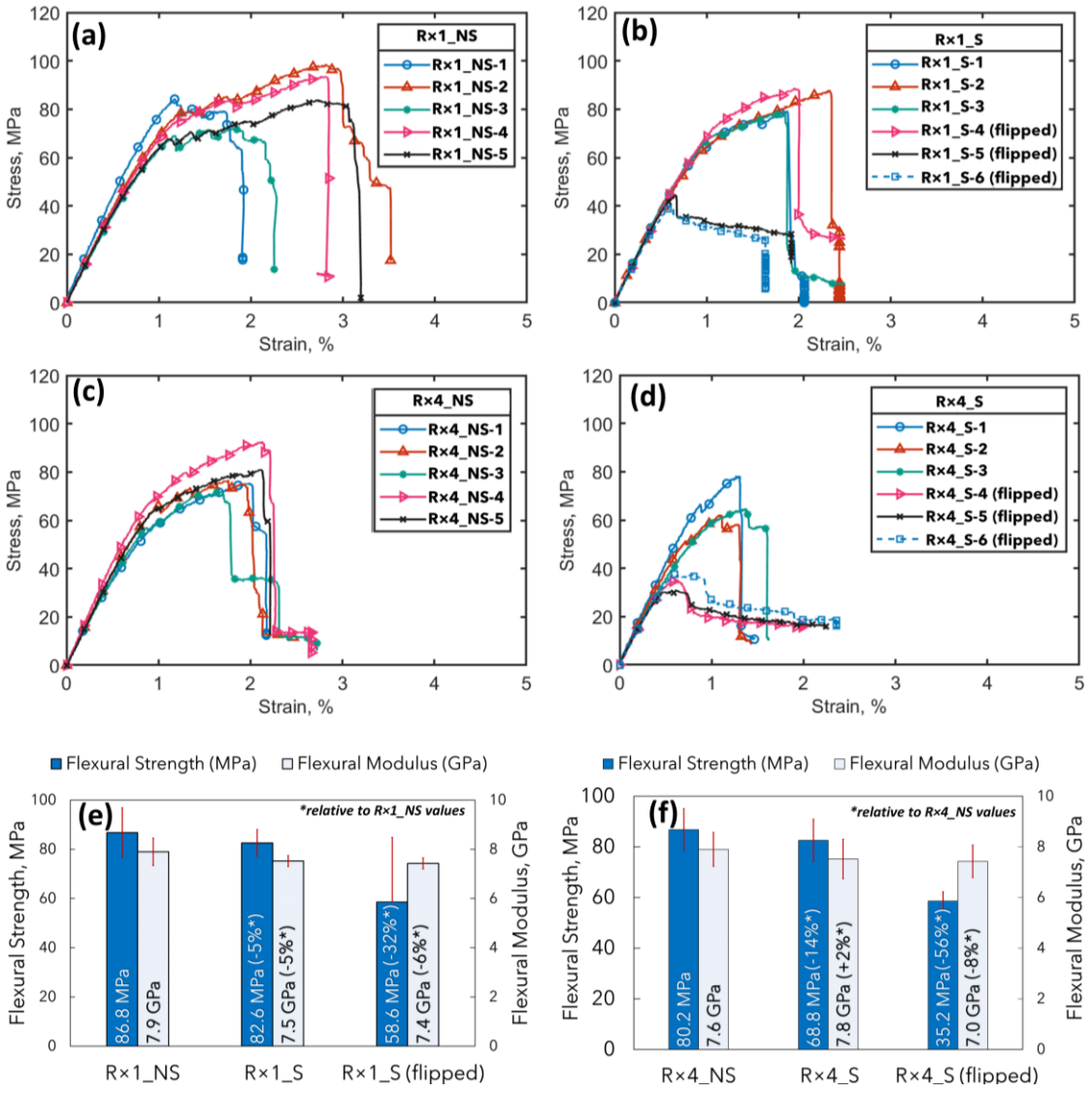

Figure 6. Stress-strain curves showing the effects of thermal reshaping on (a), (c) seam-free and seam-containing (b), (d) glass fibre-reinforced composite materials. Bar charts showing the average transverse flexural strengths and moduli for (e) R×1 and (f) R×4 samples where ×1 and ×4 indicate the number of reprocessing cycles. NS and S indicate the absence and presence of seams in the samples, respectively. Fibre volume fractions for R×1 and R×4 are 47.9% and 48.6%, respectively.

While all samples appear to exhibit the same linear stress-strain evolution Figure 6 (a)-(c), unflipped *seam* samples (R×1_S-1, R×1_S-2, and R×1_S-3) and (R×4_S-1, R×4_S-2, and R×4_S-3): Figure 6b and Figure 6d) appear to fail at lower stresses and strains than their seam-free counterparts (R×1_NS samples).

The presence of a seam in R×1_S results in 5% reductions in both strength and modulus compared to its seam-free counterpart R×1_NS. Similarly, R×4_S samples exhibit 14% lower strength values compared to R×4_NS samples. These differences are statistically significant at $p < 0.05$ as shown in S1.3. The reductions in strength are plausibly due to the pronounced structural non-uniformities, and tow distortions within the seam-containing samples as previously shown in Figure 4. All average strengths and moduli are presented in Figure 6e.

The most considerable losses in strength resulted from flipping the samples for testing as illustrated in Figure 3. The R×1_S (flipped) and R×4_S (flipped) samples exhibited 32% and 56% lower transverse flexural strengths than the R×1_NS and R×4_NS, respectively. While these differences were statistically significant, only negligible losses (6% and 8%) were observed for corresponding modulus values. Overall, R×1_S (flipped) and R×4_S (flipped) samples (Figure 6b, Figure 6d and Figure 6e) had shorter linear stress-strain evolutions, with earlier onset of failure than all other samples, characterised by massive load drops followed by high-strain material failure events. The load drop event suggests the occurrence of 0° tow rupture and/or delamination propagation within these samples. These findings suggest that strategic redesign for reuse must not only account for the presence of seams resulting from complex geometries but must factor in the orientations employed during reforming operations and subsequent re-application. Such considerations will even be more crucial for constructions using longitudinal reinforcements, where kinking and geometrical distortions can have catastrophic effects.

3.2. Dynamic mechanical analysis

Dynamic mechanical analysis (DMA) has been used to assess any microstructural changes within the polymer matrix to complement the investigations discussed in Section 3.4. For instance, any increase in crosslink density within crosslinked polymers can be revealed by an increase in the glass transition temperature (T_g) and a decrease in the loss factor (tan delta) [29,30]. The DMA thermograms obtained for this work are presented in Figure 7a-Figure 7c.

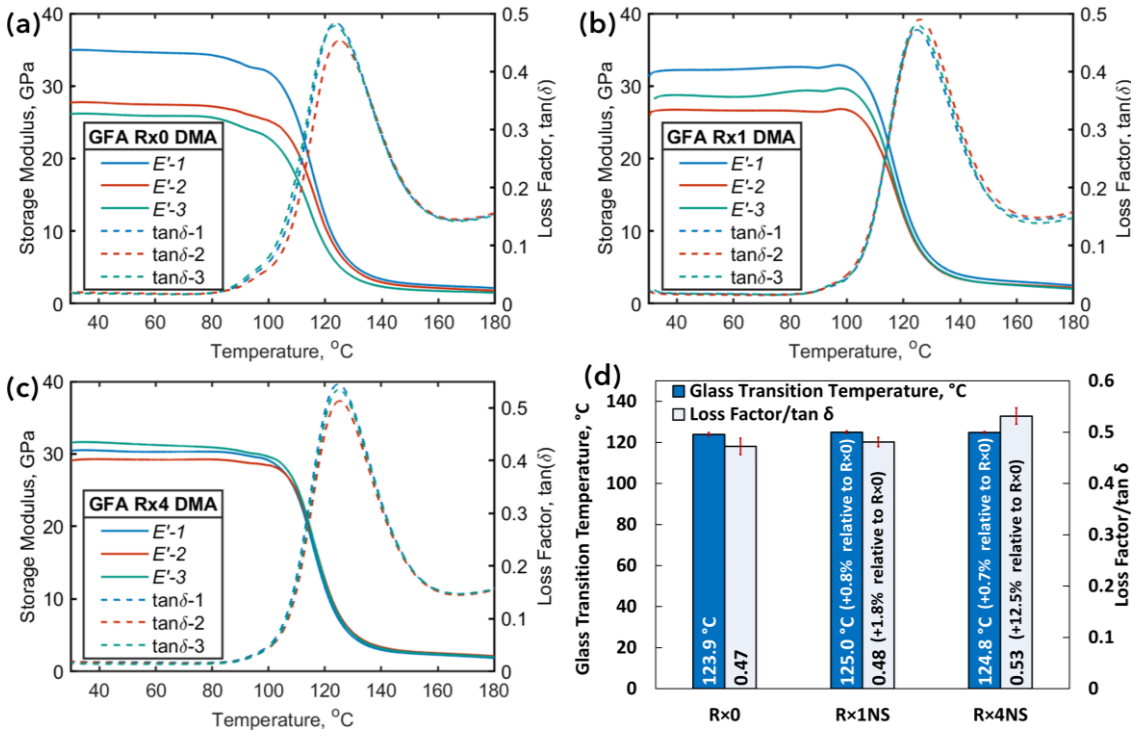

Figure 7. Dynamic mechanical analysis thermograms showing the evolution of storage moduli (E') and loss factor (tan delta) with temperature for (a) virgin R×0, and the hot-press reprocessed (b) R×1 and (c) R×4 glass fibre-reinforced acrylic materials; and (d) a bar chart showing the average glass transition temperatures and loss factor/tan delta as functions of the number of reprocessing cycles (0, 1 and 4). Fibre volume fractions for these materials in order of increasing reprocessing cycles are 47.4%, 47.9% and 48.6%.

Apart from slight changes to the apparent repeatability across the triplicates within the three sets of materials, no significant changes in T_g were observed as a result of reprocessing, with values of 124°C-125°C measured for all materials. As shown in Figure 7d, only marginal increases of 0.8% and 0.7% were measured in T_g for the R×1 and R×4 materials relative to the virgin reference (R×0), respectively. The corresponding increases in the tan delta peak of 1.8% and 12.5% suggest the unlikeliness of cross-link formation as a result of thermo-oxidative degradation of the matrix during the hot-press reprocessing steps.

3.3. Thermogravimetric analysis

3.3.1. Dynamic thermogravimetric analysis to evaluate stability

Taken together with the graphical legend in Figure 8, Table 2 presents an overview of the results shown in Figure S1 from thermogravimetric analysis of glass fibre-reinforced acrylic materials. Although the samples differ by the number of reprocessing cycles (0, 1, and 4), all samples underwent a similar degradation process to that of the unreinforced acrylic matrix of identical composition (under a nitrogen

atmosphere) as reported in the authors' previous work [17]. The interested reader may refer to the TGA results for "A100/P0" in the cited study.

From the results presented in Table 2, it can be seen that while no discernible trends were observed for the temperatures corresponding to mass losses of 5% and 10% for all sets, clear trends can be seen in the onset and endset temperatures, and residual masses.

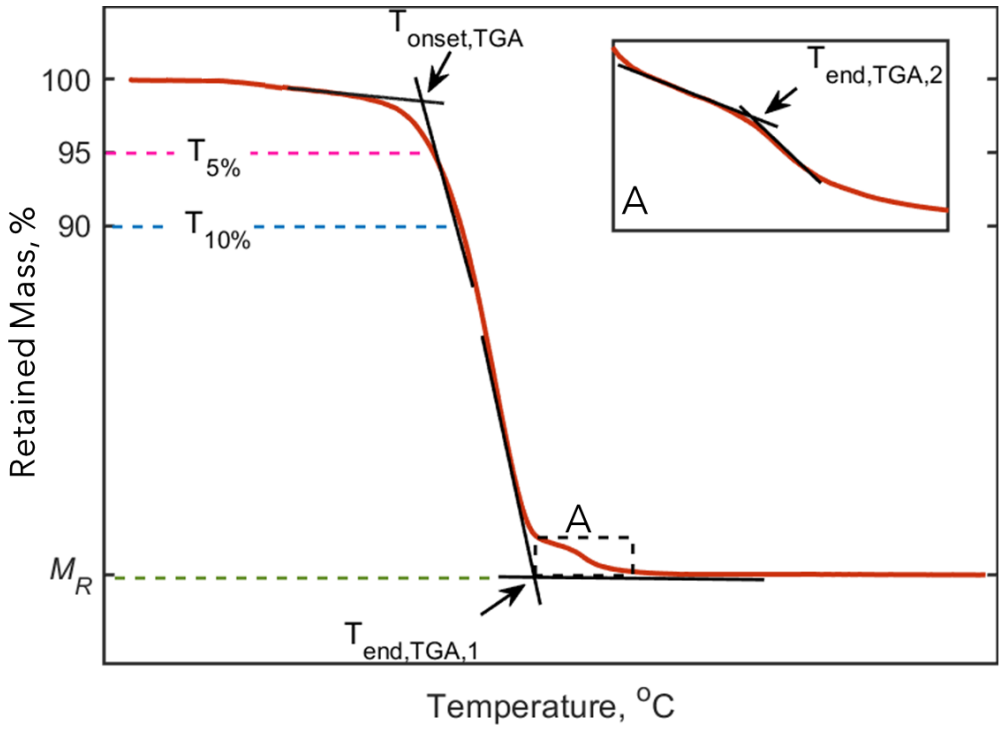

Figure 8. Idealised scheme of a TGA thermogram, showing the parameters of interest reported within this work as presented in Table 2.

Where trends exist, only marginal changes occur for all parameters. Increasing the number of reprocessing cycles appears to decrease the onset temperature by 5% from 285°C (R×0) to 270°C (R×4). Conversely, the endset temperature increases by up to 4% and the residual mass increases from 56% to 65%.

Table 2. Thermogravimetric analysis results for glass fibre-reinforced acrylic composites subjected to 0, 1 and 4 hot-press reprocessing cycles. Refer to Figure 8 for a graphical legend of the presented data.

	$T_{onset,TGA}$	$T_{5\%}$	$T_{10\%}$	$T_{end,TGA,1}$	$M_R(\%)$
R×0	285±0	279±0.5	301±1.2	376±0	56±0.1
R×1	280±0.1	276±1.4	297±1.3	381±0.9	56±0.4
R×4	270±3	278±5	301±3.8	392±4.7	65±1.5

285 Note, that the fibre mass fractions (determined using the burn-off method) for the R×0, R×1, and R×4
286 laminates were 67±0.6%, 67.4±0.4, and 68.1±0.3, respectively. Any deviation from these values may be
287 attributed to minor differences in the samples owing to the small sample quantities (approx. 15 mg) required
288 for TGA investigations. Thus, these results suggest that all three materials are virtually identical from a
289 thermal stability point of view and that reprocessing does not appear to have any deleterious effects in this
290 regard.

291 *3.3.2. Isothermal thermogravimetric simulations of extended reprocessing*

292 TGA-based simulations of extended thermal reprocessing were performed to explore the limits of
293 reprocessing with glass fibre-reinforced acrylic composites. The results of cyclic and prolonged isothermal
294 experiments are presented in Figure 9.

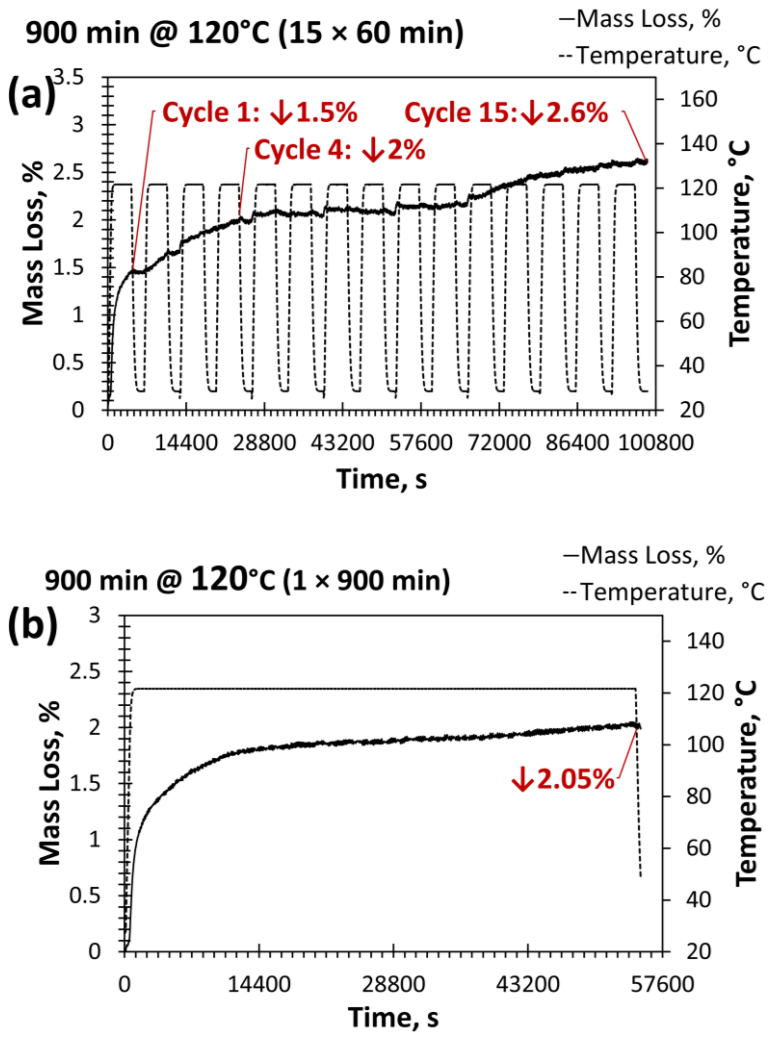

Figure 9. Results of isothermal thermogravimetry simulations of (a) successive cycles and (b) a single prolonged thermal reprocessing.

Beginning with the cyclic simulation, the corresponding mass losses for processing these materials in air can be predicted. After 1 processing cycle at 120°C for 1 hour, a mass loss of 1.5% can be expected; similarly, the 4-cycle and 15-cycle losses are predicted to be 2% and 2.6%, respectively. There appears to be a distinct transition stage of mass loss associated with the cyclic processing scheme (Figure 9a), characterised by a plateau at about 2% mass loss between Cycles 4 and 10. This stage precedes the final stage for this duration, where a further 0.6% of mass loss occurred. Interestingly, the cumulative mass loss predicted is slightly higher than that resulting from prolonged isothermal heating at 120°C for the same duration as the isothermal phases of the cyclic experiment (Figure 9a); only 2.05% is predicted to occur.

It is likely that beyond 10 cycles, some microstructural changes begin to occur due to thermal degradation. It is worth mentioning, however, that the magnitudes of mass loss reported here are still relatively low.

3.4. Solution-state nuclear magnetic resonance (NMR) spectroscopy and size exclusion chromatography (SEC)

To evaluate if the thermal reshaping affected the chemical structure of the acrylic matrix of the samples, they were analysed by solution-state NMR spectroscopy in $CDCl_3$ and SEC in THF. The acrylic matrix was removed from the glass fibres by dissolution in chloroform. . The solvent was subsequently evaporated and the recovered polymer was dissolved in $CDCl_3$ (NMR) and THF (SEC) respectively, prior to analysis. No significant solubility differences were observed between the samples when dissolving the polymer from the fibres, and all were soluble in chloroform, acetone and THF at room temperature. Cross-linked polymers typically demonstrate lower solubility than their non-cross-linked counterparts, and thus the comparable solubilities suggest that no cross-linking occurred under the thermal reshaping conditions. It is important to note that here, both SEC and NMR are used as solution-state analyses, thus only investigate the soluble components of the samples. However, visual examination showed freely floating glass fibres, indicating that no major polymeric fractions remained undissolved. Overall, these analyses provide complementary solution-state analysis of the matrix, the results of which align with the thermal and thermomechanical characterisation of the solid samples.

NMR spectroscopy is a technique that gives information on the different chemical functional groups present within the polymer structure. The solution-state ^{1}H NMR spectra of the virgin and reprocessed samples were consistent with those observed for the acrylic matrix in previous work by the authors [17], there was evidence of the BPO initiator (Figure 10). No significant differences were observed between the ^{1}H NMR spectra of the processed and unprocessed samples, which suggests that no significant structural changes have occurred. Traces of unknown species were also present, which may originate from impurities in starting materials and sample preparation, as well as small traces of the acrylic monomer (**Figure S2**), potentially due to the polymerisation becoming diffusion limited at high conversions.

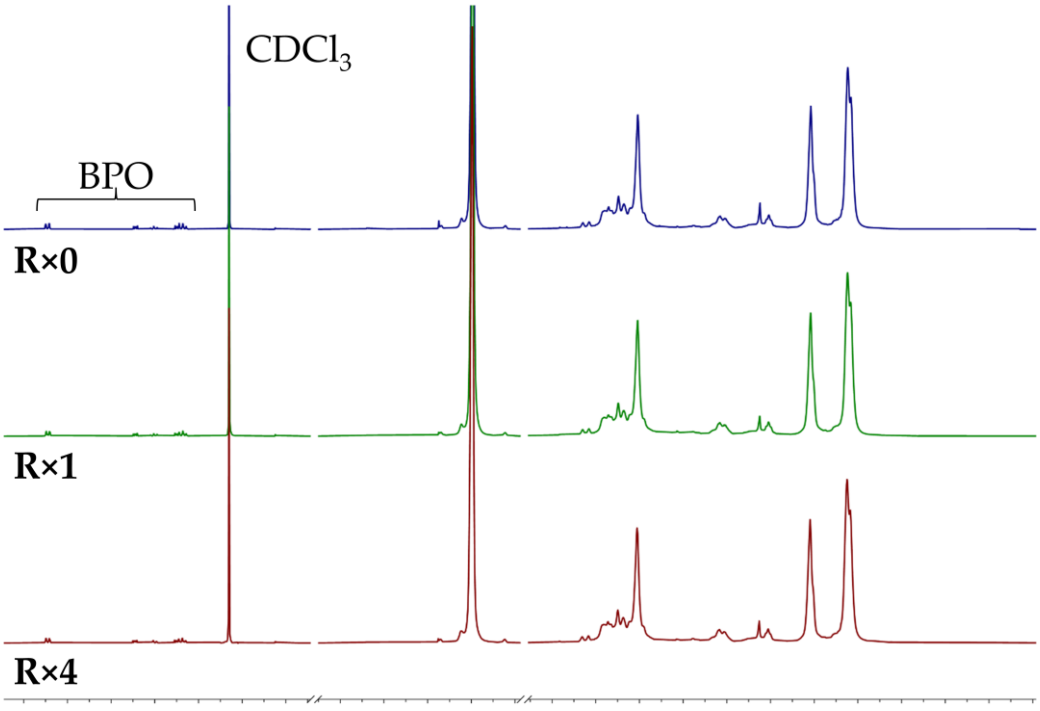

Figure 10. Overlaid ^{1}H NMR spectra of polyacrylic samples that were virgin (R×0),or reprocessed once (R×1) or four times (R×4) in $CDCl_3$.

To further confirm the absence of structural change, the samples were also analysed by 2D DOSY NMR spectroscopy. DOSY NMR is a spectroscopic technique that separates components in a mixture according to their diffusion coefficient, D. The rate at which molecules diffuse through a solution is linked to their hydrodynamic radius, and thus enables insight into the relative molecular weights of polymers [31] due to the linear relationship between the logarithm of the diffusion coefficient (logD) and the molecular weight ($\log M_w$). Introducing an average of even just one cross-link per polymer would double the molecular weight; this would lead to significant differences in diffusion times, which can be seen in DOSY NMR analysis. The spectra demonstrated that all three samples had comparable diffusion coefficients (**Figures S3 – S5**), supporting the conclusion that the acrylic matrix was not significantly affected by thermal reshaping. This was further probed by SEC analysis, as any potential cross-linking or degradation would impact molecular weights (increased or decreased respectively). The normalised SEC traces of all samples show a bimodal distribution (**Figure S6**), common for radical polymerisations of acrylic monomers[32–34].

No significant differences were observed in the molecular weights upon thermal reshaping (Table 3). Detailed analysis revealed greater variation within the same sample than was observed between the virgin

and reprocessed samples (**Figure S3** and **Tables S2 – S4**). It should be noted that SEC separates polymers based on their hydrodynamic volume rather than absolute molecular weight. It could therefore be conceivable that a cross-linked polymer could appear at comparable molecular weights to a non-cross-linked polymer due to the cross-links decreasing the hydrodynamic volume and therefore appearing smaller. The lack of differences in solubility, however, would support no cross-linking occurring. Taken together, the similar solubilities of the non-processed (R×0) and thermally reprocessed (R×1 and R×4) samples, combined with the lack of significant differences observed in the solution-state ^{1}H NMR spectroscopy, DOSY and SEC analysis suggests that no significant chemical changes have occurred in the acrylic matrix.

Table 3. SEC results for virgin acrylic matrix sample R×0 compared against thermally reprocessed samples R×1 (reprocessed once) and R×4 (reprocessed four times).

Sample[a]	M_n x 10^3 (g mol^{-1})	M_w x 10^3 (g mol^{-1})	Đ
R×0[b]	93.0	397.4	4.3
R×1[b]	87.5	413.6	4.7
R×4[b]	88.6	427.0	4.8

[a] Acrylic matrices isolated from fibres by dissolving in chloroform, filtering and drying. Samples were run in THF at 35 °C at 1 mL min^{-1} and calibrated against polystyrene standards.

[b] These results are all within experimental error of each other. See the Supplementary material, **Figure S6** and **Tables S2 – S4** for more detail.

3. Conclusions

In this study, the effects of hot-press reprocessing as a means of reusing end-of-life glass fibre-acrylic composites were examined using an *L*-shaped laminate (90° bend) The laminate was flattened incrementally between platens heated at 120°C and re-processed thermally up to 4 times. Specimens were extracted from flat regions of the original and flattened/re-processed laminates. Additionally, the effects of including a seam from the flattened components with complex geometries were comprehensively assessed. To investigate the effects of the successive reprocessing cycles on the reclaimed material's properties, three conditions of reuse were studied: a virgin reference (R×0), and two laminates subjected to 1 (R×1) and 4 (R×4) reprocessing cycles at 120°C under pressure (11 bar). Transverse flexural testing was performed along with TGA, and DMA. It was found that increasing the number of cycles results in higher transverse flexural strengths and moduli of up to 13% and 9% relative to the reference. No significant changes (<5%) were observed in the thermal stability of the reprocessed materials in the air. The glass transition temperature was maintained across the set at 125°C, whereas tan delta increased by up to 12.5%.

The possible changes in the chemical structure of the re-processed acrylic matrix were investigated with solution-state NMR and SEC. ^{1}H and DOSY NMR spectroscopy, and SEC analysis confirmed that no significant chemical change occurred under the three conditions employed in this work. Further insights were garnered from the results of simulated extended reuse studies via TGA. Cycling the glass fibre-reinforced acrylic material at 120°C for 60 minutes over 15 cycles revealed that 1-cycle and 4-cycle reprocessing can be expected to cause 1.5% and 2% mass losses, respectively. It was predicted that up to 10 cycles can be performed with negligible change in mass loss. From Cycles 10 to 15, however, a further 0.6% loss may be observed. These findings highlight unique opportunities for low-temperature, high-value reuse by thermally reshaping end-of-life continuous fibre-reinforced acrylic composites, providing insights into the associated effects on performance and limits of applicability – vital elements for realising environmental and economic benefits in the composites value chain.

Acknowledgements

The authors wish to thank the Supergen ORE Hub for funding received through the Flexible Fund Award FF2021-1014. We would also like to acknowledge the following funding sources: EPSRC SOFI2 Centre for Doctoral Training and Croda (A. L. EP/S023631/1); UKRI Future Leaders Fellowship (J. A. G. MR\T042710\1).

4. References

[1] Obande W, Ó Brádaigh CM, Ray D. Continuous fibre-reinforced thermoplastic acrylic-matrix composites prepared by liquid resin infusion – A review. Compos Part B Eng 2021. https://doi.org/https://doi.org/10.1016/j.compositesb.2021.108771.

[2] Mativenga PT, Sultan AAM, Agwa-Ejon J, Mbohwa C. Composites in a Circular Economy: A Study of United Kingdom and South Africa. Procedia CIRP, vol. 61, 2017. https://doi.org/10.1016/j.procir.2016.11.270.

[3] Joustra J, Flipsen B, Balkenende R. Circular design of composite products: A framework based on insights from literature and industry. Sustain 2021;13. https://doi.org/10.3390/su13137223.

[4] Khalid MY, Arif ZU, Ahmed W, Arshad H. Recent trends in recycling and reusing techniques of different plastic polymers and their composite materials. Sustain Mater Technol 2022;31. https://doi.org/10.1016/j.susmat.2021.e00382.

[5] Evens T, Bex GJ, Yigit M, De Keyzer J, Desplentere F, Van Bael A. The influence of mechanical

406 recycling on properties in injection molding of fiber-reinforced polypropylene. Int Polym Process
407 2019;34. https://doi.org/10.3139/217.3770.

408 [6] Rani M, Choudhary P, Krishnan V, Zafar S. A review on recycling and reuse methods for carbon
409 fiber/glass fiber composites waste from wind turbine blades. Compos Part B Eng 2021;215.
410 https://doi.org/10.1016/j.compositesb.2021.108768.

411 [7] Meng F, Cui Y, Pickering S, McKechnie J. From aviation to aviation: Environmental and financial
412 viability of closed-loop recycling of carbon fibre composite. Compos Part B Eng 2020;200.
413 https://doi.org/10.1016/j.compositesb.2020.108362.

414 [8] Liu W, Huang H, Zhu L, Liu Z. Integrating carbon fiber reclamation and additive manufacturing
415 for recycling CFRP waste. Compos Part B Eng 2021;215.
416 https://doi.org/10.1016/j.compositesb.2021.108808.

417 [9] Fernández A, Santangelo-Muro M, Fernández-Blázquez JP, Lopes CS, Molina-Aldareguia JM.
418 Processing and properties of long recycled-carbon-fibre reinforced polypropylene. Compos Part B
419 Eng 2021;211. https://doi.org/10.1016/j.compositesb.2021.108653.

420 [10] Utekar S, V K S, More N, Rao A. Comprehensive study of recycling of thermosetting polymer
421 composites – Driving force, challenges and methods. Compos Part B Eng 2021;207.
422 https://doi.org/10.1016/j.compositesb.2020.108596.

423 [11] Pender K, Yang L. Regenerating performance of glass fibre recycled from wind turbine blade.
424 Compos Part B Eng 2020;198. https://doi.org/10.1016/j.compositesb.2020.108230.

425 [12] Job S, Leeke G, Mativenga PT, Oliveux G, Pickering S, Shuaib NA. Composites recycling : Where
426 are we now ? Compos UK 2016.

427 [13] Bhudolia SK, Joshi SC, Bert A, Di YB, Makam R, Gohel G. Flexural characteristics of novel carbon
428 methylmethacrylate composites. Compos Commun 2019;13:129–33.
429 https://doi.org/10.1016/j.coco.2019.04.007.

430 [14] Bhudolia SK, Gohel G, Fai LK, Barsotti RJ. Investigation on ultrasonic welding attributes of novel
431 carbon/Elium®composites. Materials (Basel) 2020;13:10–5. https://doi.org/10.3390/ma13051117.

432 [15] Obande W, Ray D, Ó Brádaigh CM. Viscoelastic and drop-weight impact properties of an acrylic-
433 matrix composite and a conventional thermoset composite – A comparative study. Mater Lett
434 2019;238. https://doi.org/10.1016/j.matlet.2018.11.137.

435 [16] Kazemi ME, Shanmugam L, Chen S, Yang L, Yang J. Novel thermoplastic fiber metal laminates
436 manufactured with an innovative acrylic resin at room temperature. Compos Part A Appl Sci Manuf
437 2020;138:106043. https://doi.org/10.1016/j.compositesa.2020.106043.

438 [17] Obande W, Gruszka W, Garden JA, Wurzer C, Ó Brádaigh CM, Ray D. Enhancing the solvent

resistance and thermomechanical properties of thermoplastic acrylic polymers and composites via reactive hybridisation. Mater Des 2021;206:109804. https://doi.org/10.1016/j.matdes.2021.109804.

[18] Kazemi ME, Shanmugam L, Li Z, Ma R, Yang L, Yang J. Low-velocity impact behaviors of a fully thermoplastic composite laminate fabricated with an innovative acrylic resin. Compos Struct 2020;250:112604. https://doi.org/10.1016/j.compstruct.2020.112604.

[19] Pantelelis N, Bistekos E, Emmerich R, Gerard P, Zoller A, Gallardo RR. Compression RTM of reactive thermoplastic composites using microwaves and cure monitoring. Procedia CIRP 2020;85:246–51. https://doi.org/10.1016/j.procir.2019.10.005.

[20] de Andrade Raponi O, Barbosa LCM, de Souza BR, Ancelotti Junior AC. Study of the influence of initiator content in the polymerization reaction of a thermoplastic liquid resin for advanced composite manufacturing. Adv Polym Technol 2018;37:3579–87. https://doi.org/10.1002/adv.22142.

[21] Gebhardt M, Chakraborty S, Manolakis I, Meiners D. Closed-loop room temperature recycling of Elium CFRPs and its influence on the 2nd generation composite properties. J Sci Alliance Plast Technol 2020;16:179–210.

[22] Gebhardt M, Manolakis I, Chatterjee A, Kalinka G, Deubener J, Pfnür H, et al. Reducing the raw material usage for room temperature infusible and polymerisable thermoplastic CFRPs through reuse of recycled waste matrix material. Compos Part B Eng 2021;216:108877. https://doi.org/10.1016/j.compositesb.2021.108877.

[23] Bel Haj Frej H, Léger R, Perrin D, Ienny P, Gérard P, Devaux JF. Recovery and reuse of carbon fibre and acrylic resin from thermoplastic composites used in marine application. Resour Conserv Recycl 2021;173. https://doi.org/10.1016/j.resconrec.2021.105705.

[24] Cousins DS, Suzuki Y, Murray RE, Samaniuk JR, Stebner AP. Recycling glass fiber thermoplastic composites from wind turbine blades. J Clean Prod 2019;209:1252–63. https://doi.org/10.1016/j.jclepro.2018.10.286.

[25] Bennet L, Hailey J, Lomoro P, Fitzgerals A, Fuller J, Lightfoot J. Sustainable Decommissioning: Wind Turbine Blade Recycling. 2020. https://doi.org/10.13140/RG.2.2.15202.86723.

[26] De Kok JMM, Peijs T. Deformation, yield and fracture of unidirectional composites in transverse loading. 2. Influence of fibre-matrix adhesion. Compos Part A Appl Sci Manuf 1999;30. https://doi.org/10.1016/S1359-835X(98)00171-7.

[27] Liu Z, Lei Y, Zhang X, Kang Z, Zhang J. Effect Mechanism and Simulation of Voids on Hygrothermal Performances of Composites. Polymers (Basel) 2022;14. https://doi.org/10.3390/polym14050901.

[28] Tan W, Naya F, Yang L, Chang T, Falzon BG, Zhan L, et al. The role of interfacial properties on the intralaminar and interlaminar damage behaviour of unidirectional composite laminates: Experimental characterization and multiscale modelling. Compos Part B Eng 2018. https://doi.org/10.1016/j.compositesb.2017.11.043.

[29] Bandzierz K, Reuvekamp L, Dryzek J, Dierkes W, Blume A, Bielinski D. Influence of network structure on glass transition temperature of elastomers. Materials (Basel) 2016;9. https://doi.org/10.3390/MA9070607.

[30] Bao RY, Jiang WR, Liu ZY, Yang W, Xie BH, Yang MB. Balanced strength and ductility improvement of in situ crosslinked polylactide/poly(ethylene terephthalate glycol) blends. RSC Adv 2015;5. https://doi.org/10.1039/c5ra02575c.

[31] Li W, Chung H, Daeffler C, Johnson JA, Grubbs RH. Application of 1H DOSY for facile measurement of polymer molecular weights. Macromolecules 2012;45. https://doi.org/10.1021/ma301666x.

[32] Suzuki Y, Mishima R, Matsumoto A. Bulk polymerization kinetics of methyl methacrylate at broad temperature range investigated by differential scanning calorimetry. Int J Chem Kinet 2022. https://doi.org/10.1002/kin.21564.

[33] Charlier Q, Fontanier J-CC, Lortie F, Pascault J-PP, Gerard J-FF. Rheokinetic study of acrylic reactive mixtures dedicated to fast processing of fiber-reinforced thermoplastic composites. J Appl Polym Sci 2019;136:1–9. https://doi.org/10.1002/app.47391.

[34] O'Shaughnessy B, Yu J. Autoacceleration in Free Radical Polymerization. 2. Molecular Weight Distributions. Macromolecules 1994;27. https://doi.org/10.1021/ma00096a033.